

Studies of Interaction between Propranolol and Human Serum Albumin in the Presence of DMMP by Molecular Spectroscopy and Molecular Dynamics Simulation

F.S. Mohseni-Shahri^{a,*}, M.R. Housaindokht^{a,*}, M.R. Bozorgmehr^b and A.A. Moosavi-Movahedi^c

^aDepartment of Chemistry, Faculty of Science, Ferdowsi University of Mashhad, Mashhad, Iran

^bDepartment of Chemistry, Mashhad Branch, Islamic Azad University, Mashhad, Iran

^cInstitute of Biochemistry & Biophysics, University of Tehran, Tehran, Iran

(Received 25 November 2015, Accepted 10 January 2016)

ABSTRACT

The interaction between propranolol (PROP) and human serum albumin (HSA) was studied in the presence of dimethyl methylphosphonate (DMMP). DMMP is usually considered as a simulant for chemical warfare agents (CWAs). For this purpose fluorescence quenching, resonance light scattering (RLS), synchronous, three-dimensional fluorescence spectroscopy and molecular dynamics (MD) simulation were employed under physiological conditions. Fluorescence spectroscopy showed that DMMP could quench, and PROP increased intensity of the HSA fluorescence spectra. The presence of DMMP remarkably decreased binding constant of PROP to HSA. Therefore, by decreasing the amount of drugs transported to its target, the free drug concentration of the target would be raised, increasing the efficacy of the drug. The results of synchronous fluorescence and three-dimensional fluorescence spectra showed that the binding of PROP and DMMP to HSA induced conformational changes of HSA. According to molecular dynamics simulation results proposed that these ligands could interact with the HSA, with affecting the secondary structure of protein and with a modification of its tertiary structure.

Keywords: Human serum albumin, Dimethyl methylphosphonate, Propranolol, Molecular dynamics simulation, Fluorescence quenching

INTRODUCTION

Organophosphorus anticholinesterases (OPs) are in the most toxic substances identified [1,2]. Originally, OPs were developed for utilize as insecticides [3], but their excessive toxicity toward higher vertebrates because of their capability to inhibit acetylcholine esterase (AChE) has led to their adoption as weapons of warfare [3,4]. The OPs are tabun (GA), sarin (GB), soman (GO), cyclosarin (GF), VX (O-ethyl S [2-(diisopropylamino)ethyl]methyl phosphonothionate) and VR (N,N-diethyl-2-(methyl-(2-methyl-propoxy)phosphoryl)sulfanylethanamine) [3,5]. Due to the toxicity of nerve agents and usage limitations, research on the CWAs is often conducted using compounds with similar chemical structures but being non-toxic, named stimulants [6]. Dimethyl methylphosphonate (DMMP, CH₃PO

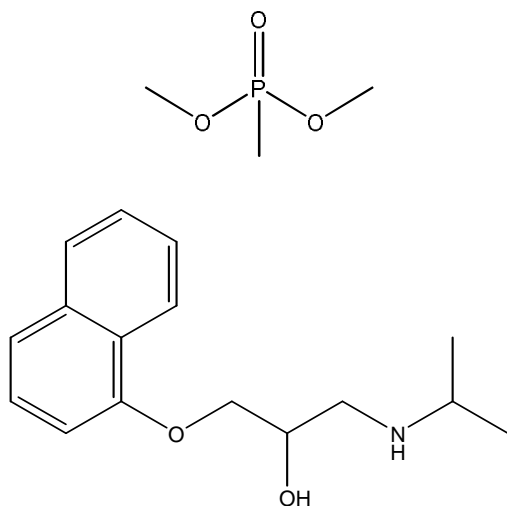
(OCH₃)₂) (Scheme 1a) because of its organophosphorus composition mimics nerve agents is usually considered as a simulant for chemical warfare agents (CWAs), such as the G-series nerve agents [7].

Human serum albumin (HSA) is the most abundant protein in the blood. This globular protein, which consists of a single polypeptide chain of 585 amino acid residues, has important physiological functions, including in the transport and distribution of many molecules and metabolites, such as fatty acids, amino acids, hormones, cations and anions and many drugs.

HSA is also known to bind OPs and to react with them [8,9]. OPs are actually hydrolyzed by albumin through transient phosphorylation/alkylation of its active site [10]. The residue that reacts with organophosphates was investigated to be a tyrosine [11].

Propranolol (Inderal) (1-isopropylamino-3-(1-naphthoxy)-2-propanol) (Scheme 1b) is an important beta-adrenergic blocking agent and employed in the management

*Corresponding authors. E-mail: housain@um.ac.ir; fmohsenishahri@gmail.com



Scheme 1. Chemical structure of (a) DMMP and (b) Propranolol.

of hypertension angina pectoris and cardiac dysrhythmias [12]. It has been shown that the distribution, free concentration, and metabolism of various drugs can be significantly altered because of their binding to HSA [13].

Using chemical warfare agents (CWAs) as a weapon of terrorism has become an actual existing threat. The enormous repeated uses of nerve agents during Iran-Iraq war in the 1980s against civilians by Iraqi troops and during terrorist attacks in the 1990s by the Aum Shinrikyo sect in Japan emphasize the constant danger. In the work presented here, we investigate *in vitro* the interaction of PROP and DMMP with HSA, as well as to evaluate the competition between the binding of PROP in the presence of DMMP by various techniques. The results obtained from this study would be important to demonstrate the interactions between HSA and PROP in chemical ulcerous.

EXPERIMENTAL AND COMPUTATIONAL METHODS

Materials

Fatty acid free HSA and DMMP were used as received from Sigma-Aldrich® Chemical Company (St. Louis, USA). PROP was obtained from Tehran-Darou Company (Iran). All salts used for buffer preparation were of analytical grade and were dissolved in double distilled water. HSA, PROP

and DMMP were dissolved in a phosphate buffer (pH = 7.4, 50 mM), and the concentrations were 7.5×10^{-3} mM, 6.47×10^{-2} mM and 4.8×10^{-2} mM, in all techniques used, respectively. In measurements for each data point, 50 μ l of DMMP and PROP solution were added to 2.5 ml of the HSA solution and using a micro syringe to attain a series of final concentrations ($0-1.11 \times 10^{-2}$ mM) for the binary and ternary systems.

INSTRUMENTATIONS

All fluorescence measurements were carried out in a Jasco FP-6200 (Hitachi Japan) spectrofluorometer at room temperature (25 ± 1 °C), using quartz cell with 1cm optical path length, and both bandwidths were set at 5 nm. The fluorescence spectra were then measured (the excitation wave lengths were 280 nm and the emission wave lengths were 300-500 nm). Synchronous fluorescence spectra were acquired by simultaneously scanning the excitation and emission monochromators. Such synchronous fluorescence spectra only show the Tyr and Trp residues of HSA when the wavelength interval ($\Delta\lambda$) is 15 and 60 nm, respectively.

Resonance light scattering (RLS) spectra were obtained by simultaneously scanning both the excitation and the emission monochromators with $\Delta\lambda = 0$ nm [14], from 220-700 nm, with the same instrument used for the fluorescence measurements. Three-dimensional fluorescence spectra were obtained on the initial excitation wavelength was set at 220 nm with increments of 10 nm, and the emission wavelength was recorded from 220-500 nm with increments of 1 nm. The scan rate was set to 500 nm min⁻¹. The absorption spectra were performed on a Shimadzu-UV2550 UV-Vis spectrophotometer equipped with quartz cells. All pH measurements were performed with a pH-meter WTW 537.

Molecular Dynamics Simulation Details

All calculations were carried out by Gromacs software version 4.5.4 [15] and the GROMOS 43a1 force field. It is exhibited that the experimental observations of the protein conformations and stability are reproduced by GROMOS force field in aqueous [16] and non-aqueous phase [17]. Moreover, comparing GROMOS force field with other biomolecular force fields showed that GROMOS commonly

delivered the better representation of the experimentally observed structural behavior of the proteins [18]. Three simulation boxes in $6.8 \times 6.6 \times 8.1 \text{ nm}^3$ dimensions were designed and HSA (pdb code: 1AO6) was placed in box centers. 100 molecules of DMMP were respectively placed in the first simulation box, 50 PROP molecules and 50 DMMP molecules were put inside the second box and no drug was added to the third one. Since PROP and DMMP potential parameters are not defined in Gromacs software, PRODRG [19] web server was used to assign these parameters in the framework of GROMOS force field. In order to use this web server optimized structure of the interested molecule is needed. The geometry of PROP and DMMP were optimized by the DFT (B3LYP/6-31G (d)) method of the Gamess software [20]. Then all simulation boxes were filled with simple point charge (SPC) water. For having neutral conditions in terms of electrical charge, suitable number of ions is added to each box. To minimize the energy of considered system and to relax water and ions steepest-descent algorithm was performed. Molecular dynamics simulation was carried out in two stages. In the first stage, position-restrain simulation was conducted in which the atoms of the protein molecule were held fixed, whereas the water molecules and ions were free to move around, so that they would reach the equilibrium state. In the second stage, each system is simulated with a time step of 2 fs. A 20 ns MD simulation was performed for the protein in each solvent. Linear constraint solver (LINCS) algorithm [21] was employed to fix the chemical bonds between the atoms of the protein and SETTLE [22] algorithm in the case of solvent molecules. The atoms in the systems were given initial velocities according to Maxwell-Boltzmann distribution at 300 K. To maintain a constant temperature and pressure for various components during simulations, the V-rescale coupling algorithm was used [23]. For each component of the systems particle mesh Ewald (PME) algorithm was applied to estimate the electrostatic interactions. In this algorithm, every atom interacts with all the other atoms in the simulation box and with all of their images in an infinite array of periodic cells; so, satisfactory results are produced from the electrostatic interactions [24].

RESULTS AND DISCUSSION

Fluorescence Measurements

In general, the intrinsic fluorescence of HSA is caused by tryptophan and tyrosine because phenylalanine has a very low quantum yield [25]. According to literature; fluorescence spectroscopy is widely used for investigating the interactions between drugs and proteins [26].

The presence of DMMP causes the quenching of fluorescence of HSA. Fluorescence quenching is the decrease of the quantum yield of fluorescence from a fluorophore caused by a variety of molecular interactions, such as ground-state complex formation, excited-state reactions, molecular rearrangements, energy transfer and collisional quenching. The different mechanisms of quenching are usually grouped as either static quenching or dynamic quenching [27]. The fluorescence spectra of HSA in the presence of DMMP at different concentrations are shown in Fig. 1a.

As can be seen in Fig. 1a, HSA exhibited a strong fluorescence emission peak at 335 nm after being excited with a wavelength of 280 nm. The fluorescence intensity of HSA shown a significant decrease with an obvious shift of the peak toward shorter wavelength (from 335-322 nm), after the addition of DMMP, this indicated that DMMP could interact with HSA and quench its intrinsic fluorescence, and the micro-environment of tryptophan residue in HSA was changed, leading to an increase of hydrophobicity in the vicinity of this residue [28]. To determine the fluorescence quenching mechanism, the well-known Stern-Volmer equation was utilized for the data analysis [29]:

$$\frac{F_0}{F} = 1 + K_q \tau_0 [Q] = 1 + K_{sv} [Q] \quad (1)$$

where F_0 and F are the fluorescence intensities in the absence and presence of quencher, respectively; K_q is the quenching rate constant of the biomolecule, K_{sv} is the Stern-Volmer dynamic quenching constant, τ_0 is the average lifetime of the fluorophore without quencher ($\tau_0 = 10^{-8}$ s), and $[Q]$ is the concentration of quencher.

The inset of Fig. 1a shows the Stern-Volmer curve for the binding of DMMP with HSA. HSA has a maximum

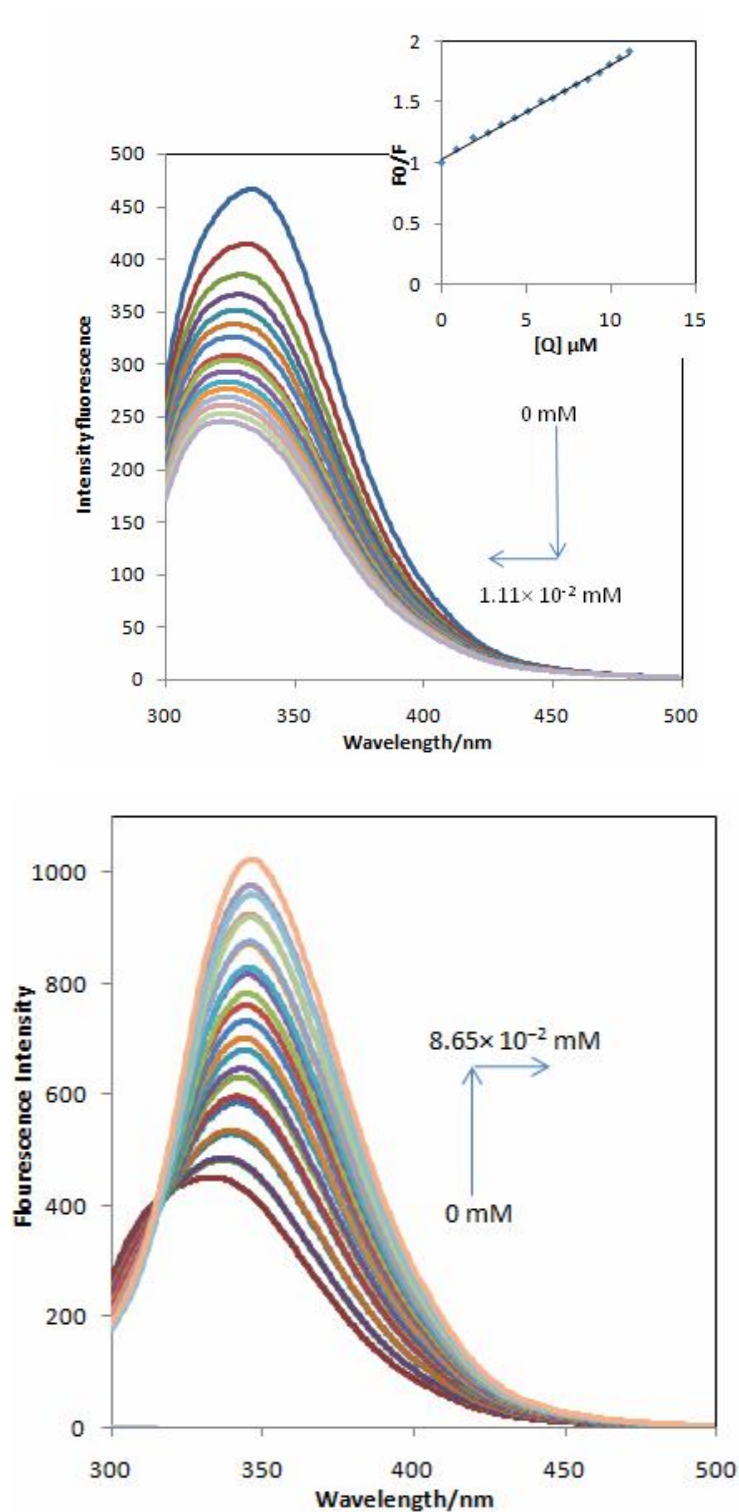


Fig. 1. Fluorescence emission spectra of the protein-ligand systems in the presence of various concentrations of ligands for the (a) HSA-DMMP system (inset: The Stern-Volmer plots of HSA by DMMP), (b) (HSA-DMMP)-PROP system, ($\lambda_{ex} = 280$ nm, pH = 7.4, T = 298 K).

fluorescence emission at around 340 nm, while DMMP has no intrinsic fluorescence at around this wavelength. Upon additions of DMMP, the fluorescence intensity of HSA decreased, so the successive binding of DMMP should occur close to the tryptophan residue. The corresponding K_{SV} value for the interaction between DMMP and HSA was obtained to be $8.6 \times 10^4 \text{ M}^{-1}$ (298 K, $R^2 = 0.996$). The value of K_q was calculated to be $8.6 \times 10^{12} \text{ M}^{-1} \text{ s}^{-1}$ (298 K). The value of K_q was much greater than the limiting diffusion rate constant of the biomolecule ($2 \times 10^{10} \text{ M}^{-1} \text{ s}^{-1}$), which suggested that the quenching mechanism of HSA by DMMP is static quenching [30]. The tryptophan fluorescence from HSA was corrected for an inner filter effect. PROP has the strong absorption peaks in the excitation wavelength of HSA [31]. To obtain the proper fluorescence intensity values, fluorescence data must be corrected for the inner filter effect caused by attenuation of the excitation beam and emission signal because of absorption by quencher and fluorophore. These absorption events lead to artificial decrease in the fluorescence intensities; this effect is corrected using the equation [32]:

$$F_c = F * \text{anti} \log \left\{ \frac{A_{ex} + A_{em}}{2} \right\} \quad (2)$$

Where F and F_c are experimentally measured and corrected fluorescence intensities, respectively, A_{ex} and A_{em} are the absorbance of PROP at the emission and excitation wavelength, respectively. It is known that propranolol exhibits intrinsic fluorescence in the ultraviolet region with a solvent-dependent maximum between 320 and 360 nm [33]. In the absence of DMMP, the fluorescence intensity of HSA increased regularly upon interaction with PROP and the red shift was observed for the emission wavelength. The shift in maximum wavelength towards longer wavelengths (red shift) suggests that binding PROP to HSA caused micro-environmental changes in HSA and the Trp-214 residue of HSA suited to a more polar (or less hydrophobic) environment, and the protein was unfolded [34]. Figure 1b shows the fluorescence intensity of HSA by PROP in the presence of DMMP, excited at 280 nm. The fluorescence of HSA-DMMP was increased upon interaction with PROP. The shift in maximum wavelength for the ternary system was believed to be due to the conformational changes

induced by the interactions. The appearance of an isobestic point at 318 nm might also indicate the existence of equilibrium between bound and free drug. In addition, such equilibrium may emphasize the formation of the drug protein complex [35].

Estimation of the Binding Constants

Since for HSA-DMMP system, the fluorescence quenching was a result of a static quenching mechanism, the binding constant (K_a) and the number of binding sites (n) can be determined by the following equation:

$$\frac{\log((F_0 - F))}{F} = \log K_a + n \log Q \quad (3)$$

A plot of $\log((F_0 - F)/F)$ vs. $\log[Q]$ gave a straight line using least squares analysis, and its slope was equal to n (binding affinity) with an intercept on the Y-axis of $\log K_a$ [36]. After analyzing the data with the Hill equation, the values of n and K_a could be obtained, and they are listed in Table 1.

In (HSA-DMMP)-PROP system where fluorescence enhancing occurred, the fraction saturation (θ) was used [37]:

$$\frac{F - F_0}{F_\infty - F_0} = \theta \quad (4)$$

Where F_0 , F and F_∞ are corrected fluorescence intensities of HSA in the absence and presence of the PROP, and at the saturation, respectively. Therefore, the following equation was improved [38]:

$$\frac{1}{F - F_0} = \frac{1}{F_\infty - F_0} + \left(\frac{1}{K_a [Q]} \right) \left(\frac{1}{F_\infty - F_0} \right) \quad (5)$$

Where K_a is the binding constant and $[Q]$ is the drug concentration. A plot of $1/(F - F_0)$ vs. $1/[Q]$ yield the binding constant as the slope. The linearity in the plot of $1/(F - F_0)$ against $1/[Q]$ confirms a one-to-one interaction between the two partners. In our previous study it has been shown that the binding constant of PROP to HSA is $0.87 \times 10^5 \text{ M}^{-1}$ (without inner filter effect correction) and $1.14 \times 10^5 \text{ M}^{-1}$ (with inner filter effect correction) [34], as shown in Table 1, the binding constant was decreased in the presence of DMMP (HSA-DMMP)-PROP system.

Table 1. Estimated Values of the Binding Constant (K_a) and Binding Site (n) for Binary and Ternary Systems at $\lambda_{ex} = 280$ nm (pH 7.4, T = 298 K)

System	K_a ($\times 10^{-5} \text{ M}^{-1}$)	n	R^2
HSA-DMMP	0.78	0.919	0.996
HSA-PROP [33]	1.14	1.000	0.995
(HSA-DMMP)-PROP	0.87	1.000	0.995

Synchronous Fluorescence Spectroscopy Studies

The molecular environment in the vicinity of a fluorophore was investigated by synchronous fluorescence spectroscopy. As displayed in supplementary Fig. S1 for (HSA-DMMP)-PROP complex, the emission maximum of Trp residue was red-shifted, which demonstrated that the polarity of the fluorophore increased, causing the hydrophobic cavities to be moved to a more hydrophilic environment. Moreover, the maximum emission wavelength of the Tyr residues did not have a significant shift, which implies that the interaction of PROP with HSA in the ternary system did not affect the conformation of the region around the Tyr residues [39].

To investigate the structural change of HSA caused by the addition of PROP in the presence of DMMP, measurements were made of curves of F/F_0 vs. [PROP] (supplementary Fig. S2) with various amounts of PROP (at $\Delta\lambda = 60$ and $\Delta\lambda = 15$ nm). Results displayed a higher slope when $\Delta\lambda$ was 60 nm, indicating a significant contribution of Trp residue of HSA in the ternary system, and PROP closer to Trp residue as compared to Tyr residues. Indeed, the structure of the micro-environment of the Trp residue was altered by PROP in the absence [34] and the presence of DMMP.

RESONANCE LIGHT SCATTERING

RLS is a highly sensitive and selective method for the study of aggregation and assembly of chromophores on biological macromolecules [40]. In recent years; this technique has been developed for the determination of

proteins. By scanning both the excitation and emission monochromators of a common spectrofluorometer with $\Delta\lambda = 0$ nm, RLS spectra can be recorded and have proven to be practical when investigating the aggregation of small molecules [41].

The RLS spectra of (HSA-DMMP)-PROP complex is recorded by synchronous scanning from 220-700 nm with $\Delta\lambda = 0$ nm (data are not shown). After addition of ligand, a strong wide RLS band can be observed, indicating that the interaction between HSA and PROP in the presence of DMMP has occurred. The increase of RLS intensity is correlated with the formation of certain aggregation and is controlled mainly by the particle dimension of the formed aggregation in solution [42]. It is concluded from the results that the DMMP and PROP may interact with HSA in solution.

Three-dimensional Fluorescence Spectra

Three-dimensional fluorescence spectroscopy has been commonly applied for studying the interaction between small molecules and proteins in recent years. The outstanding advantage of the method is that it can provide more detailed information about the conformational change of protein by simultaneously changing excitation and emission wavelengths. Emission wavelength, excitation wavelength and fluorescence intensity can be used as the axes, making the probing of the characteristic conformational changes of proteins more scientific and reliable [43].

The three-dimensional spectra and contour map of the (HSA-DMMP)-PROP complex are presented in Fig. 2 and

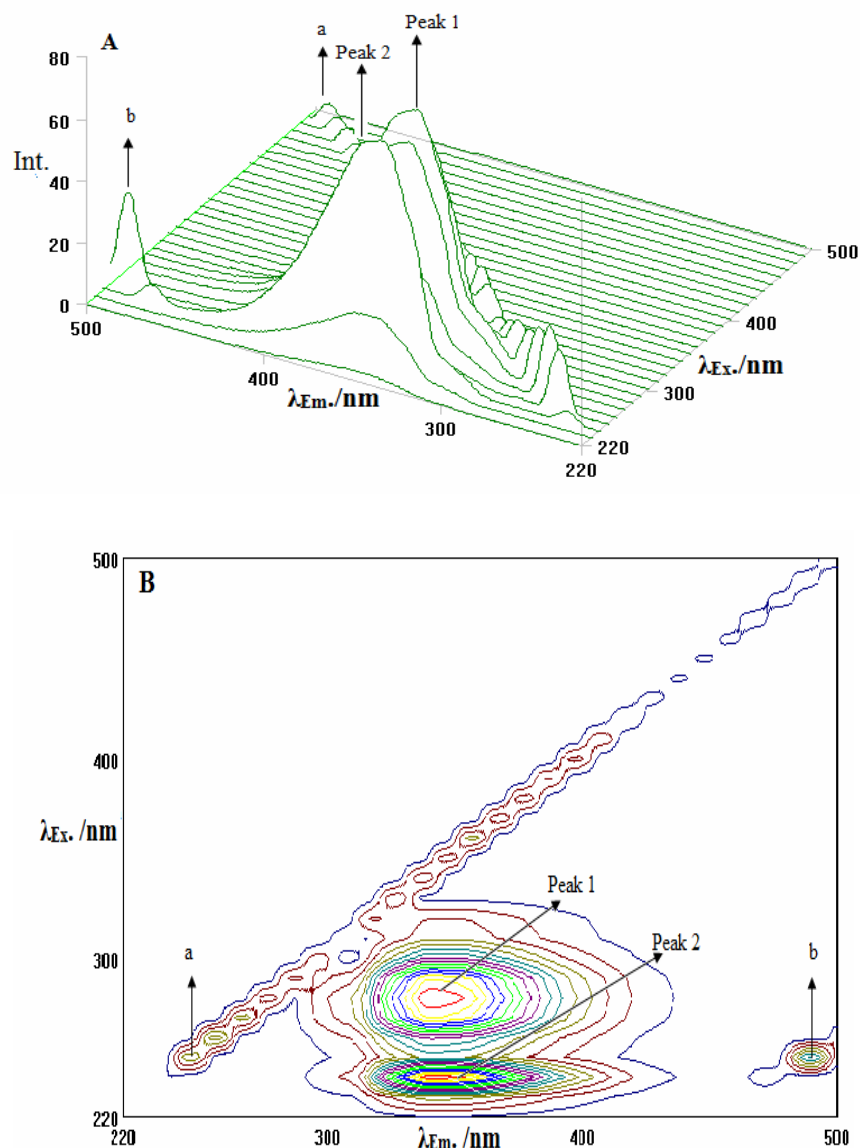


Fig. 2. Three-dimensional fluorescence spectra and corresponding contour maps of (a and b) (HSA-DMMP)-PROP (pH = 7.4, T = 298 K).

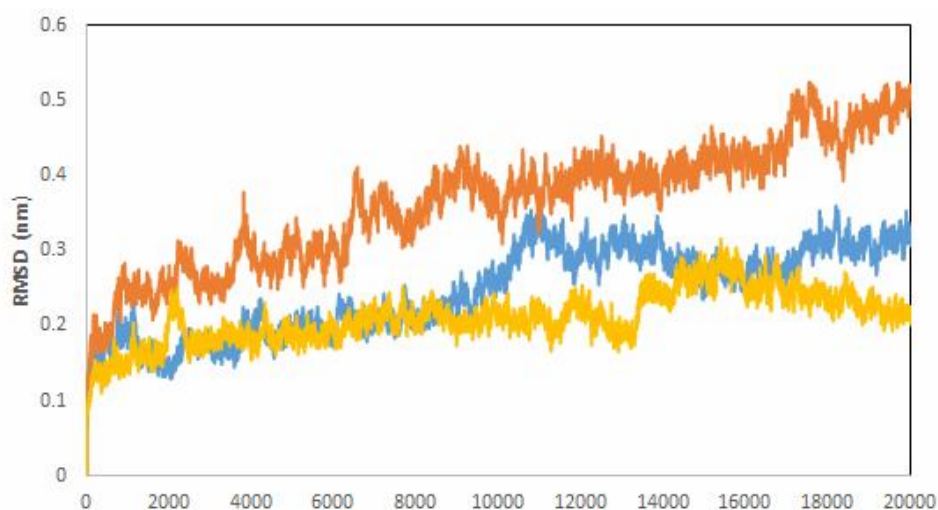
corresponding characteristic parameters are listed in Table 2. According to the Fig. 2, peak a is the first-ordered Rayleigh scattering peak ($\lambda_{ex} = \lambda_{em}$), and peak b is the second-order scattering peak ($\lambda_{ex} = 2\lambda_{em}$), which is principally caused by the $\pi \rightarrow \pi^*$ transition of the characteristic polypeptide backbone structure C=O of HSA. Peak 1 ($\lambda_{ex} = 280$ nm, $\lambda_{em} = 340$ nm) reveals the spectral characteristic of Trp and Tyr residues; Peak 2 ($\lambda_{ex} = 230$

nm, $\lambda_{em} = 340$ nm) relates to the spectral behavior of polypeptide backbone structure, and its fluorescence intensity is mutually related to the secondary structure of protein [44].

It was clear that both fluorescence peaks 1 of HSA have been increased by DMMP and PROP, although to different measures. This was evidence of complex formation between ligands and HSA in the binary and ternary systems, causing

Table 2. Three-dimensional Fluorescence Spectral Characteristics of HSA and HAS-ligand in all Interacting Systems (pH 7.4, T = 298 K)

System	Peak1 ($\lambda_{ex}/\lambda_{em}$)	$\Delta\lambda$ (nm)	Intensity	Peak2 ($\lambda_{ex}/\lambda_{em}$)	$\Delta\lambda$ (nm)	Intensity
HSA	280/336	56	24.94	230/331	101	4.00
HSA-DMMP	280/338	58	23.18	230/338	108	2.94
HSA-PROP [33]	280/342	62	91.89	230/343	113	32.98
(HSA-DMMP)-PROP	280/342	62	74.96	230/342	112	19.057

**Fig. 3.** RMS deviation of distance between alpha-carbon atoms from the crystal structure as a function of simulation time for free HSA (red), HSA-DMMP (yellow) and HSA-DMMP-PROP (blue).

a change in the conformation of HSA. In addition, the results showed that the micro-environment had undergone consequential alterations during formation of the HSA-DMMP and (HSA-DMMP)-PROP complexes and the structure of HSA had been changed by the binding of ligands [45].

Molecular Dynamics Simulation

Molecular dynamics (MD) is a method to visualize the structural changes of a protein over a defined time scale. Nowadays, molecular dynamics simulation is a powerful and strong tool to calculate the time-dependent action of a molecular system.

Root Mean Square Deviation (RMSD)

In a MD simulation, a common way to monitor the structural stability of a macromolecule is to calculate the root mean square deviation from the initial structure during the simulation. The overall RMSD, between simulated structure of HSA and the starting one, computed on C-alpha atoms, for each system, is shown in Fig. 3.

RMSD of free HSA increased quickly and didn't reach to equilibrium until 20 ns and it showed much larger RMSD values. In the HSA-DMMP and HSA-PROP [33] systems the RMSD of back bone atoms steadily increased to about 0.2 nm and then stabilized around 15 ns and remained stable till the end of the simulation. In the ternary system the

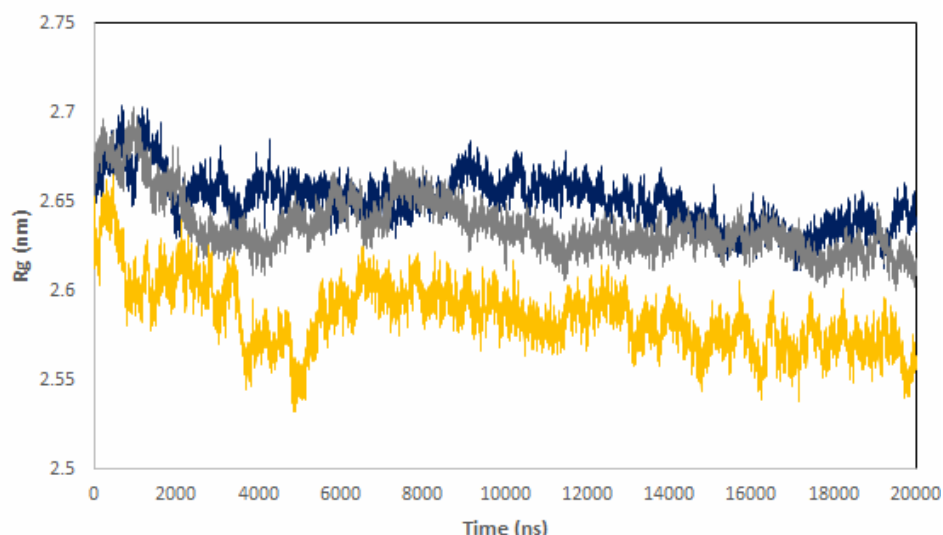


Fig. 4. Radiuses of gyration as a function of time for free HSA (yellow), HSA-DMMP (dark) and HSA-DMMP-PROP (gray).

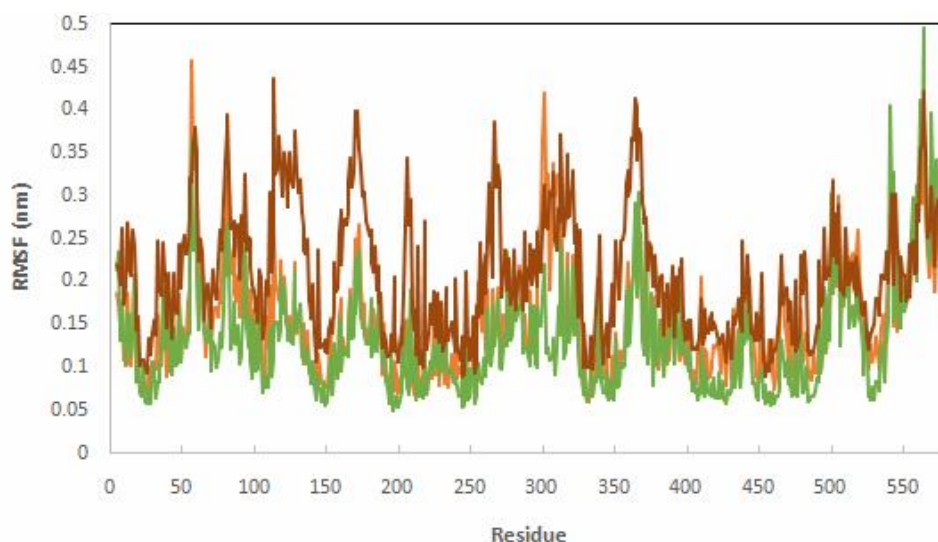


Fig. 5. Root mean squared fluctuation over residues numbers for free HSA (red), HSA-DMMP (orange) and HSA-DMMP-PROP (green).

RMSD of back bone atoms reached to about 0.25 nm and then stabilized around 18 ns. These results show the protein structures have undergone changes on interaction with ligands in binary and ternary systems. Thus, the protein shows higher conformational stability in HSA-liganded than free HSA.

Radius of Gyration (R_g)

Figure 4 shows the gyration radius variations for protein during the simulation. The graph displays The binding of PROP [33] and DMMP to HSA were found to increase the R_g in the binary and ternary systems. It could be clearly seen that the radius of gyration of HSA increases on binding of

the ligands implying a less compact structure and partial unfolding of the protein after the simulation. This indicates that ligand binding changes the microenvironment of HSA leads to the conformational changes in the HSA during MD simulation. These R_g values are strongly supported with the experimental fluorescence data.

Root Mean Square Fluctuations (RMSF)

Local protein mobility was analyzed by calculating the time averaged RMSF values of free HSA, HSA-DMMP and HSA-PROP-DMMP systems were plotted against residue numbers based on the 20 ns trajectory data shown in Fig.5.

Most regions of HSA were stabilized in HSA-DMMP complex after binding the ligand, except residues 295-305 that have slightly higher RMSF values. This region is loop that connects helices: IIA-h6 to IIB-h1 (residues 292-314).

In the HSA-PROP-DMMP system, almost all regions of HSA were stabilized after binding the ligands, except residues 536-544 and 562-565 that have higher RMSF values. In these residues the second structure of protein was changed and the coil-helix transformation was occurred (the second structure of free HSA and HSA-liganded were shown in Supplementary Figs. S3-S5), whereas, in the absence of DMMP, there is a region, including residues 505-515 that shows higher flexibility than that of the free HSA [34]. In general, the results indicate that the secondary structure of the protein was altered during the simulation period.

Analysis of Ligand Binding to Protein

Due to the motions of the ligand and protein molecule, the ligand could collide with different parts of the protein structure. Also the ligand will collide more frequently with binding sites on the protein structure. To explore theoretically the molecular mechanisms of ligand binding to proteins through the use of molecular dynamics simulations, firstly, the collisions of ligand molecules with every residue of HSA were evaluated. Next, the average numbers of collisions with each residue was clarified and then assessed. Subsequent, a measure of the affinity of a residue, P_i , referred to as the conformational factor, toward a ligand molecule was estimated. A residue can be counted as being indifferent toward the ligand when its P_i value turns out to be unity. The residue i with $P_i > 1$ is assumed to have

affinity toward the ligand, while with $P_i < 1$ it has no affinity [46].

The P_i values for the residues of HSA in the binary and ternary systems were calculated and the values of $P_i > 1$ are listed in Supplementary Table S1. The results reveal that the residues with the hydrophobic nature are having the $P_i > 1$ and His-440, Ile-142 and Pro-180 of the protein have the largest value of P_i in the HSA-PROP, HSA-DMMP and HSA-DMMP-PROP systems, respectively. In other words, these residues would have the greatest affinity towards ligand. A comparison between the results calculated shows that the number and type of residues with $P_i > 1$ is different in the absence and presence of DMMP. These results indicate that the protein structures have undergone changes on interaction with ligands in binary and ternary systems.

Moreover, the distance between the residues that having the largest value of P_i and the greatest affinity towards ligand with Trp 214 were about 2.12, 2.64 and 3.44 nm, in HSA-PROP, HSA-DMMP and HSA-DMMP-PROP systems, respectively.

Secondary Structure

Secondary structure is always connected with the biological activity of proteins. The components of this structure were calculated based on DSSP method to quantitatively analyze the conformational changes. Free HSA has 74.4% α -helix, in the HSA-DMMP, HSA-PROP [33] and (HSA-DMMP)-PROP, the proportions changed to 68.7, 74.6 and 66.4%, respectively.

This may suggest that, in the presence of DMMP, PROP is able to interact with the amino acid residues of the polypeptide chain of HSA, partially destroy the hydrogen bonding networks [47], bring out some degree of protein destabilization [48], and adopt a more open conformation and better exposure of hydrophobic cavities [49]. All the above analysis (Table 3) revealed that the binding of DMMP in the binary and ternary systems could cause slight conformational and some micro-environmental changes of HSA.

Residue-Residue Contact Map

Protein contact map predicts the tertiary structure of protein. Contact maps of free HSA in comparison with HSA-DMMP and HSA-PROP-DMMP were shown in

Table 3. Secondary Structural Analysis of the Binary and Ternary Systems from DSSP Method

System	%G ^a	%H ^a	%C ^a	%S ^a	%T ^a
Free HSA	0.0	74.4	13.5	6.1	6.1
HSA-DMMP	1.6	68.7	14.2	6.6	9.0
HSA-PROP [33]	0.0	74.6	13.7	6.7	5.0
HSA-DMMP-PROP	3.3	66.4	13.3	6.7	10.2

^aG, H, C, S and T are 3-helix, alpha helix, coil, bend and hydrogen bonded turn, respectively.

Table 4. Contacts with most Differences between Two Structures in Two and Three Component Systems

System	Regions with maximum differences
Free HSA in comparison with HSA-DMMP	Ala575 and Val73-Glu91, Pro109 and Cys71-Val73, Thr79 and Val529-Lys530
Free HSA in comparison with HSA-PROP-DMMP	Ala55 and Glu354-Glu364, Thr492 and Val73-Lys89, His531 and Thr72-Lys89, Ala577 and Thr72-Gln90
Free HSA in comparison with HSA-PROP [33]	Phe498 and Glu33-Asn105, Thr562 and Gln25-Asn105
HSA-PROP-DMMP in comparison with HSA-DMMP	Asp52 and Asp297-Leu298, Asp558 and Asp68-His101, Lys462 and Ala500
HSA-PROP-DMMP in comparison with HSA-PROP	Asp508 and Phe32-Ser54, Lys560 and Ser1-Ser61, Lys560 and Val116-Ile138

Supplementary Figs. S6-S7. Supplementary Figs. S8-S9 shows the contact maps of HSA-PROP-DMMP in comparison with HSA-DMMP and HSA-PROP. Maximum differences are related to the contacts are listed in Table 4. Contact maps exhibit that PROP can interact with HSA in the presence of DMMP and change its tertiary structure.

CONCLUSIONS

The interaction between PROP and HSA in the presence of DMMP was clarified at the molecular level using spectroscopy with the aid of molecular dynamics simulation under physiological conditions. The quenching mechanism of fluorescence of HSA was mainly initiated by the static mechanism. DMMP decreased the binding affinity between

the PROP and HSA in the (HSA-DMMP)-PROP system. The decrease of binding constant should shorten the retention time of the drug in blood plasma and increase its maximum effectiveness.

Synchronous fluorescence and 3D fluorescence results revealed that the secondary structure and the microenvironment of protein altered with the addition of PROP in the ternary system. The interaction of PROP with HSA resulted in an enhancement of the RLS intensity in the ternary system. MD simulation results suggested that PROP could interact with HSA in the presence of DMMP, with affecting the secondary structure of HSA and with a slight modification of its tertiary structure. This study is expected to provide important insight into the interactions of HSA with drugs in the presence of DMMP.

Supplementary Information

Figures S1-S9 and Table S1 as described in the text are included.

ACKNOWLEDGMENTS

The financial support for this work was provided by Research Council of Ferdowsi University of Mashhad (Research project no. 3/24357-91/10/12).

REFERENCES

- [1] Z. Ying, Y. Jiang, X. Du, G. Xie, J. Yu, H. Wang, *Sensor Actuat. B-Chem.* 125 (2007) 167.
- [2] S. Reutter, *Environ. Health Persp.* 107 (1999) 985.
- [3] C.P. Holstege, M. Kirk, F.R. Sidell, *Crit. Care Clin.* 13 (1997) 923.
- [4] F.R. Sidell, *Nerve Agents. Medical Aspects of Chemical Warfare.* Washington, DC: BordenInstitute, 2008.
- [5] E. Lee, *Annals of the Academy of Medicine,* Singapore, 1997.
- [6] E. Brunol, F. Berger, M. Fromm, R. Planade, *Sensor Actuat. B-Chem.* 120 (2006) 35.
- [7] S.L. Bartelt-Hunt, D.R. Knappe, M.A. Barlaz, *Crit. Rev. Env. Sci. Tec.* 38 (2008) 112.
- [8] G. Means, H.L. Wu, *Arch. Biochem. Biophys.* 194 (1979) 526.
- [9] R.M. Black, M.J. Harrison, R.W. Read, *Arch. Toxicol.* 73 (1999) 123.
- [10] M.A. Sogorb, A. Monroy, E. Vilanova, *Chem. Res. Toxicol.* 11 (1998) 1441.
- [11] C. Milstein, F. Sanger, *Biochem. J.* 79 (1961) 456.
- [12] M.A. Gotardo, J.O. Tognolli, H.R. Pezza, L. Pezza, *Spectrochim. Acta A* 69 (2008) 1103.
- [13] C.N. Yan, H.X. Zhang, P. Mei, Y. Liu, *Chinese J. Chem.* 23 (2005) 1151.
- [14] L. Li, Q. Pan, Y.X. Wang, G.W. Song, Z.S. Xu, *Appl. Surf. Sci.* 257 (2011) 4547.
- [15] E. Lindahl, B. Hess, D. Van Der Spoel, *J. Mol. Model* 7 (2001) 306.
- [16] S. Melchionna, M. Barteri, G. Ciccotti, *J. Phys. Chem.* 100 (1996) 19241.
- [17] C.M. Soares, V.H. Teixeira, A.M. Baptista, *Biophys. J.* 84 (2003) 1628.
- [18] M. Schmidt, K. Baldrige, J. Boatz, S. Elbert, M. Gordon, J. Jensen, S. Koseki, N. Matsunaga, K. Nguyen, S. Su, *J. Comput. Chem.* 14 (1993) 1347.
- [19] D. Van der Spoel, E. Lindahl, *J. Phys. Chem. B* 107 (2003) 11178.
- [20] A.W. Schuttelkopf, D.M. Van Aalten, *Acta Crystallogr. D* 60 (2004) 1355.
- [21] H. Berendsen, J. Postma, W. Van Gunsteren, J. Hermans, in: B. Pullman (Ed.), *Interaction Models for Water in Relation to Protein Hydration, Intermolecular Forces,* Reidel, Dordrecht, 1981.
- [22] T. Darden, D. York, L. Pedersen, *J. Chem. Phys.* 98 (1993) 10089.
- [23] H. Hess, H. Bekker, H.J. Berendsen, J.G. Fraaije, *J. Comput. Chem.* 18 (1997) 1463.
- [24] C. Danculescu, B. Nick, F.J. Wortmann, *Biomacromolecules* 5 (2004) 2165.
- [25] N. Zhou, Y.Z. Liang, P. Wang, *J. Mol. Struct.* 872 (2008) 190.
- [26] Y.J. Hu, Y. Liu, L.X. Zhang, R.M. Zhao, S.S. Qu, *J. Mol. Struct.* 750 (2005) 174.
- [27] X. Shi, X. Li, M. Gui, H. Zhou, R. Yang, H. Zhang, Y. Jin, *J. Lumin.* 130 (2010) 637.
- [28] T. Yuan, A.M. Weljie, H.J. Vogel, *Biochemistry* 37 (1998) 3187.
- [29] J.R. Lakowicz, G. Weber, *Biochemistry* 12 (1973) 4161.
- [30] C. Wang, Y. Li, *J. Agr. Food Chem.* 59 (2011) 8507.
- [31] B. Iacob, I. Tiuca, E. Bodoki, R. Oprean, *Farmacia* 61 (2013) 79.
- [32] J.R. Lakowicz, *Principles of Fluorescence Spectroscopy,* Plenum Press, New York, London, 1983.
- [33] R.H. Bisby, S.W. Botchway, A.G. Crisostomo, J. Karolin, A.W. Parker, L. Schroder, *Spectroscopy* 24 (2010) 137.
- [34] F.S. Mohseni-Shahri, M.R. Housaindokht, M.R. Bozorgmehr, A.A. Moosavi-Movahedi, *J. Lumin.* 154 (2014) 229.
- [35] T. Yuan, A.M. Weljie, H.J. Vogel, *Biochemistry* 37 (1998) 3187.
- [36] A. Varshney, P. Sen, E. Ahmad, M. Rehan, N. Subbarao, R.H. Khan, *Chirality* 22 (2010) 77.

- [37] Y.J. Hu, Y. Liu, Z.B. Pi, S.S. Qu, *Bioorgan. Med. Chem.* 13 (2005) 6609.
- [38] R. Subramanyam, A. Gollapudi, P. Bonigala, M. Chinnaboina, D.G. Amooru, *J. Photoch. Photobio. B* 94 (2009) 8.
- [39] Y.Q. Wang, H.M. Zhang, G.C. Zhang, Q.H. Zhou, Z.H. Fei, Z.T. Liu, Z.X. Li, *J. Mol. Struct.* 886 (2008) 77.
- [40] Z. Chen, J. Liu, Y. Han, *Talanta* 71 (2007) 1246.
- [41] W. Lu, J. Shang, *Spectrochim. Acta A* 74 (2009) 285.
- [42] S.K. Patra, A.K. Mandal, M.K. Pal, *J. Photoch. Photobio. A* 122 (1999) 23.
- [43] M. Rodríguez-Cuesta, R. Boqué, F. Rius, D. Picón Zamora, M. Martínez Galera, A. Garrido Frenich, *Anal. Chim. Acta* 491 (2003) 47.
- [44] D. Li, Y. Wang, J.B. Chen, *J. Spectrochim. Acta A* 79 (2011) 680.
- [45] G. Zhang, Q. Que, J. Pan, J. Guo, *J. Mol. Struct.* 88 (2008) 132.
- [46] M.R. Housaindokht, M.R. Bozorgmehr, M. Bahrololoom, *J. Theor. Biol.* 254 (2008) 294.
- [47] Y. Wang, X. Wang, J. Wang, Y. Zhao, W. He, Z. Guo, *Inorg. Chem.* 50 (2011) 12661.
- [48] F. Ding, J.X. Diao, Y. Sun, Y. Sun, *J. Agr. Food Chem.* 60 (2012) 7218.
- [49] X. Pan, P. Qin, R. Liu, J. Wang, *J. Agr. Food Chem.* 59 (2011) 6650.